Off-Line PD Diagnosis for Stator Winding of Rotating Machines Using a UWB Sensor

Kyaw-Soe Lwin†, Noh-Joon Park*, Hee-Dong Kim, Young-Ho Ju**, and Dae-Hee Park***

Abstract – We studied partial discharge detection by sensing electromagnetic waves emitted from the partial discharge source in an HV Rotating Machine using a UWB sensor. In this study, we design a new type of compact low frequency UWB sensor based on micro-strip technology. We also perform many experiments of offline and dismantled testing compared with the existing HFCT on stator winding of the HV generator. We mention the detailed design of a new compact UWB sensor along with the time domain PRPD pattern and frequency domain results of partial discharge in the stator winding of a 6.6kV rotating machine by offline testing performed in a laboratory.

Keywords: HV Rotating Machine, Partial Discharge, Time Domain and Frequency Domain Analysis, UWB Sensor

1. Introduction

Partial discharge testing has been used for decades as a method to evaluate the condition of insulation systems used in medium to high voltage rotating machines. Now, partial discharge testing is also rapidly becoming an industry standard as a quality assurance (QA) test for newly installed stator winding insulation systems. PD testing can be done either offline (energizing the apparatus with an external transformer) or online (where the apparatus is excited by the power system) [1]. PD testing is favourable in case of the sudden unexpected in-service failure of the stator winding insulation of large rotating machines which would cause considerable expense for non-availability and unplanned repair work. Therefore, PD diagnostic tests are applied to assess the condition of the insulation system.

The stator winding insulation of high voltage machines is subjected to several stresses such as electrical stress, thermal stress, and mechanical stress during operation that may significantly influence the performance of the insulation system and especially its long-term properties due to the various aging phenomenon. Modern insulation systems for high voltage machines are inherently resistant to the partial discharge of their inorganic mica components. The main sources of partial discharge activity in high voltage rotating machines are Voids/Delamations, Slot/Slot exit discharges, and End winding discharges [2].

† Corresponding Author: Wonkwang University, Iksan, South Korea
* Wonkwang University, Iksan, South Korea
** Korea Electric Power Research Institute, Daejeon, South Korea
Received 22 January, 2008; Accepted 2 April, 2008

During the partial discharge process, there are many forms of energy exchanges such as electrical pulse current, dielectric loss, electromagnetic radiation, sound, ultrasonics, acoustics emission, increased gas pressure, and chemical reactions. In detecting partial discharge, depending on the sensing of the kinds of energy exchange, different detecting methods were approached. In these methods, electromagnetic sensing proved to be one of the best kinds of partial discharge detection and localization of PD source.

The occurrence of partial discharges in electrical insulation is always associated with the emission of electromagnetic pulses. A typical PD pulse has a rise time less than 1ns and a pulse width of several ns, implying a frequency domain of several GHz [10]. The electromagnetic emission propagates in all directions from the PD source.

Attenuation of electromagnetic PD pulse is a function of frequency along the propagation path. The higher the frequency, the more rapidly components will be attenuated when they travel along the cable [3-4]. Therefore, the detectable electromagnetic (EM) wave emitted from the PD includes broadband signal of VHF/UHF (Very High Frequency: 30MHz to 300MHz/ Ultra High frequency: 300MHz to 3000MHz) [5].

We tried to collect ultra wideband (UWB) signals by using a new design compact low frequency UWB antenna sensor which can detect both low frequency and high frequency bands. This compact UWB antenna sensor is a modification of conventional rectangular patch antenna by adding notches based on the microstrip line antenna theory. CST MS version 5.0, microwave simulation software is

used to design and implement the UWB antenna sensor.

Off-line dismantled PD testing is deployed to test new UWB sensors to be comparative with commercial high frequency current transformers (HFCTs) in the Laboratory. Some experimental results will be discussed over HFCT sensors and our UWB antenna sensor in the detection of partial discharge in 6.6kV stator winding.

2. Sensor Design and Fabrication

2.1 Theory Background

Also called 'patch' antennas, microstrip patch antennas consist of a metallic patch that is on the top of a grounded dielectric substrate of thickness h, with relative permittivity ε_r and permeability μ_r (usually taken 1) as shown in Fig. 1.

Patch antennas are widely used in microwave frequency range but they are often used in millimetre-wave frequency range as well by modifying various shapes of patch design [10]. The metallic patch essentially creates a resonant cavity, where the patch is the top of the cavity, the ground plane is the bottom of the cavity, and the edges of the patch from the sides of the cavity.

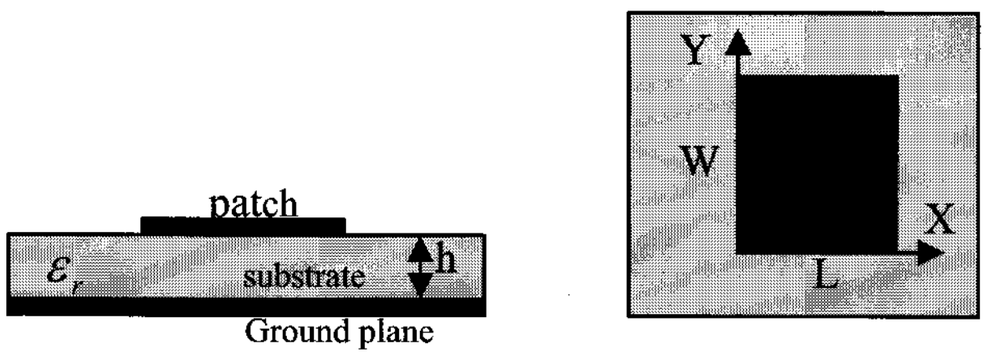

Fig. 1. Schematic diagram of patch antenna

The edges of the patch act approximately as an open-circuit boundary condition.

Hence, the patch cavity modes are described by a double index (m,n). For (m,n) cavity mode of the rectangular patch, the electric field has the form

$$E_x(x,y) = A_{mn}\cos\left(\frac{m\pi x}{L}\right)\cos\left(\frac{n\pi x}{W}\right) \quad (1)$$

where L is the patch length and W is the patch width. The patch is usually operated in the (1,0) mode, so that L is the resonant dimension and the field is essentially constant in the y direction. The resonant frequency of the (1,0) mode is given by

$$f_0 = \frac{c}{2L_e\sqrt{\varepsilon_r}} \quad (2)$$

where c is the speed of light in a vacuum. To account for the fringing of the cavity fields at the edge of the patch, the effective length Le is chosen as

$$L_e = L + 2\Delta L \quad (3)$$

The Hammerstad formula for the fringing extension is [7],

$$\Delta L/h = 0.412\frac{(\varepsilon_{eff}+0.3)(\frac{W}{h}+0.264)}{(\varepsilon_{eff}-0.258)(\frac{W}{h}+0.8)} \quad (4)$$

where

$$\varepsilon_{eff} = \frac{\varepsilon_r+1}{2} + \frac{\varepsilon_r-1}{2}(1+10\frac{h}{W})^{-1/2} \quad (5)$$

For this mode the patch may be regarded as a wide microstrip line of width W, having resonant length L, that is approximately one half-wavelength in the dielectric. The current is maximum at the centre of the patch, $x = L/2$, while the electric field is maximum at the "radiating" edges, x=0, and x=L. The width W is usually chosen to be larger than the length (W=1.5L is typical) to maximize the bandwidth, since the bandwidth is proportional to the width of the antenna bandwidth.

2.2 Sensor Design

The basis of this design is a rectangular element improved for wider bandwidth in low frequency and it can detect signals from nearby fields. The width of the patch element is chosen 1.5 times that of the resonant length and modified with two notched patches which can be operated at both low and high frequencies of ultra wideband operating. Our UWB sensor design was realized on a FR4 substrate (ε_r=4.6, thickness=1.6mm) in order to keep the cost low. At low frequencies the antenna size is the principal constraint, e.g. at 500MHz, the dimension of a $\lambda/2$ antenna is 30 cm. It is very difficult to integrate as a sensor. Therefore, to reduce the antenna size at low frequency, the patch antenna is used.

Simulation has been carried out with CST MWS version 5.0 to determine resonant bandwidth, return loss and input impedance. The rectangular patch element is fed by microstrip line access, which is a common microwave transmission line that offers fairly good performance in terms of the bandwidth, and at low cost.

To increase the antenna bandwidth, two cutting notches are used in the rectangular patch by controlling impedance stability [8]. These notches alter the electromagnetic coupling between the rectangular patch and ground plane. The width of the notches is particularly effective either at

low or high frequencies. Matching improvement can be obtained by inserting a slot in the ground plane [7]. The characteristics of the antenna highly depend on the ground plane shape. The best result can be obtained by changing ground length Lg with the ground slot of Ws.

These notches alter the electromagnetic coupling between the rectangular patch and ground plane [9]. In sensor design structure, the main rectangular patch element is modified with three notched patched elements and a microstrip line feeding method is used. Some parts of the ground region are removed and modified with the ground slot to obtain wider bandwidth.

2.3 Parameter Optimization and Simulation Results

The width of the notches is particularly effective either at low or high frequencies. Matching improvement can be obtained by inserting a slot in the ground plane [10]. The optimization parameters are W_{n1}, W_{n2}, W_f, and W_s while the feed line length L_f is fixed.

Several parameter optimizations are made by simulation to get the desired bandwidth and target frequency. An example of ground length optimization is shown in Fig. 2.

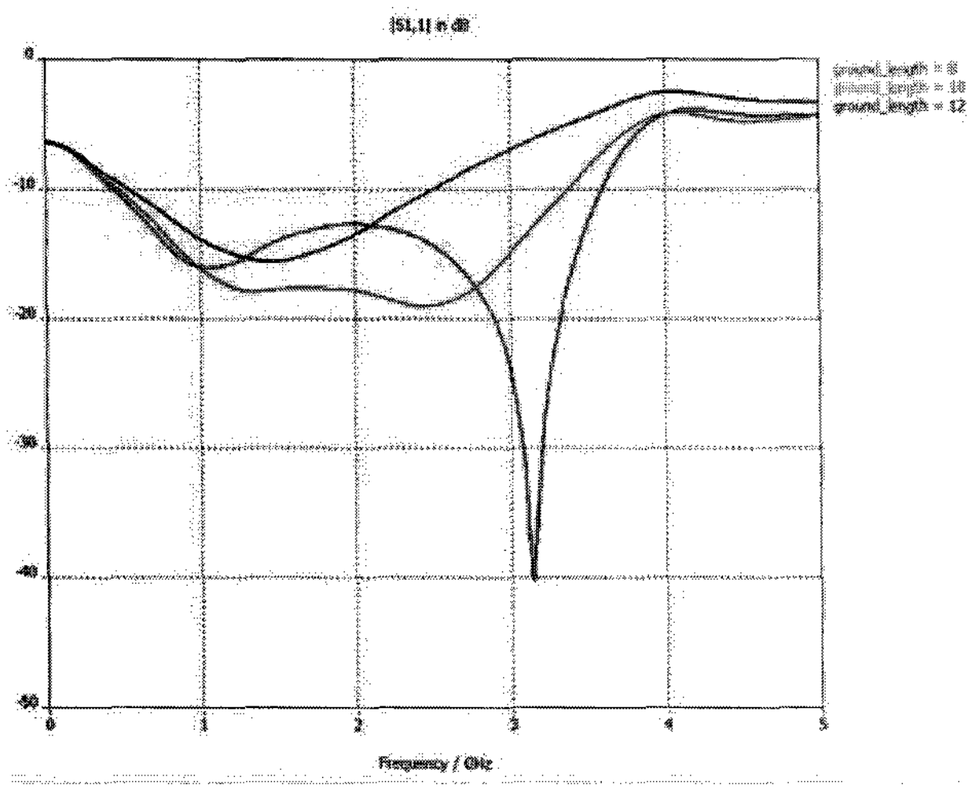

Fig. 2. Ground length optimization

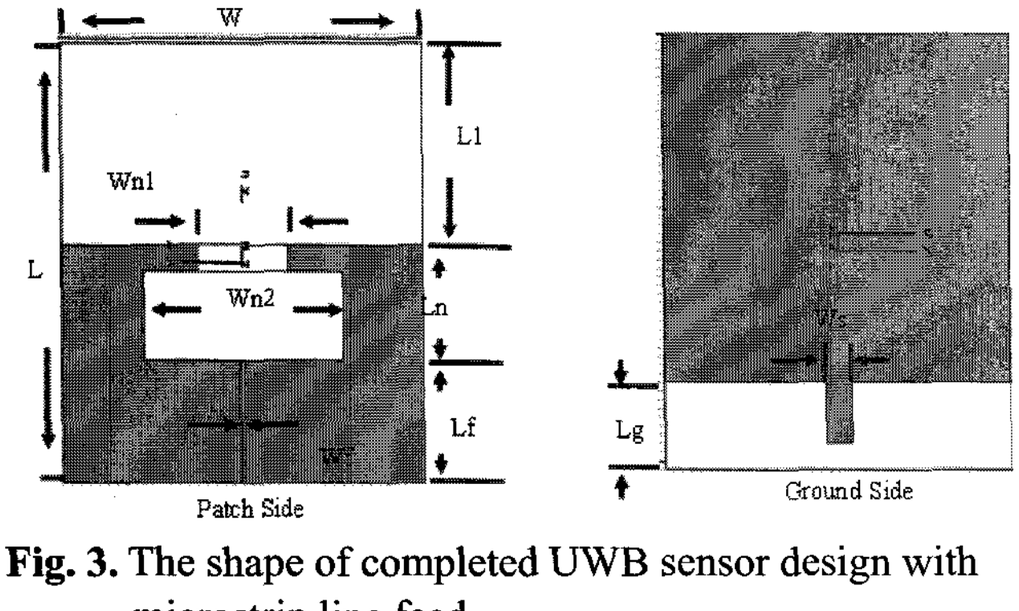

Fig. 3. The shape of completed UWB sensor design with microstrip line feed

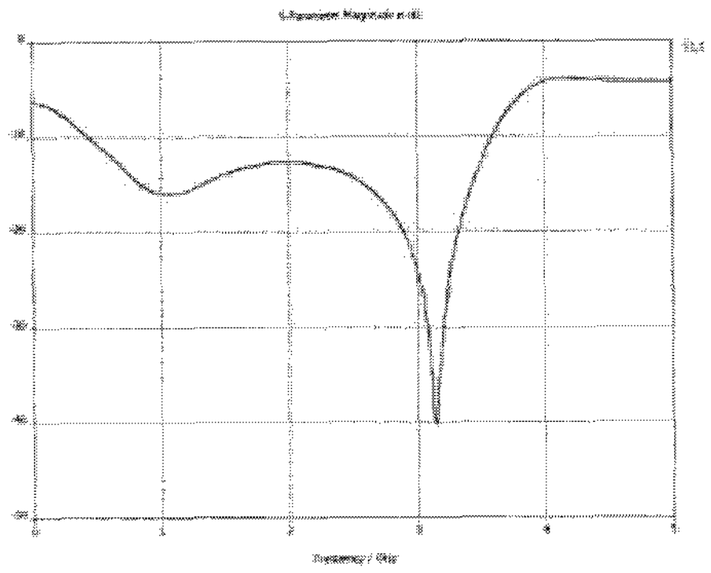

Fig. 4. The simulation result of return loss and -10 dB bandwidth

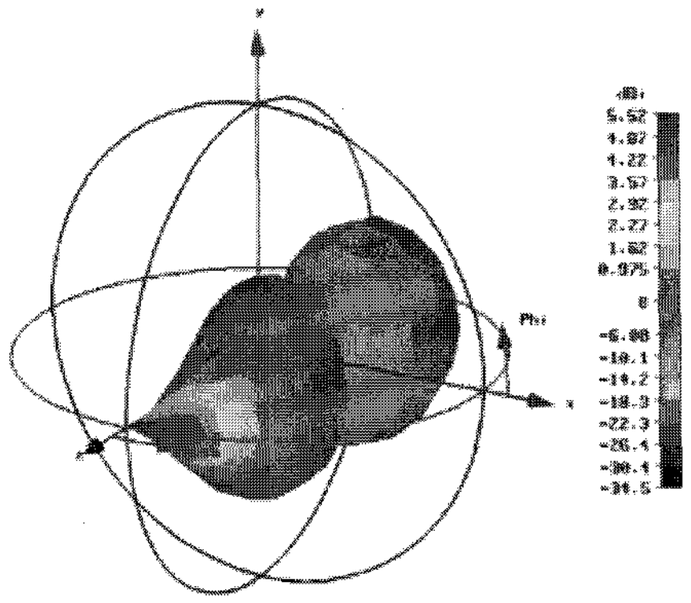

(a) Theta pattern of far-field radiation

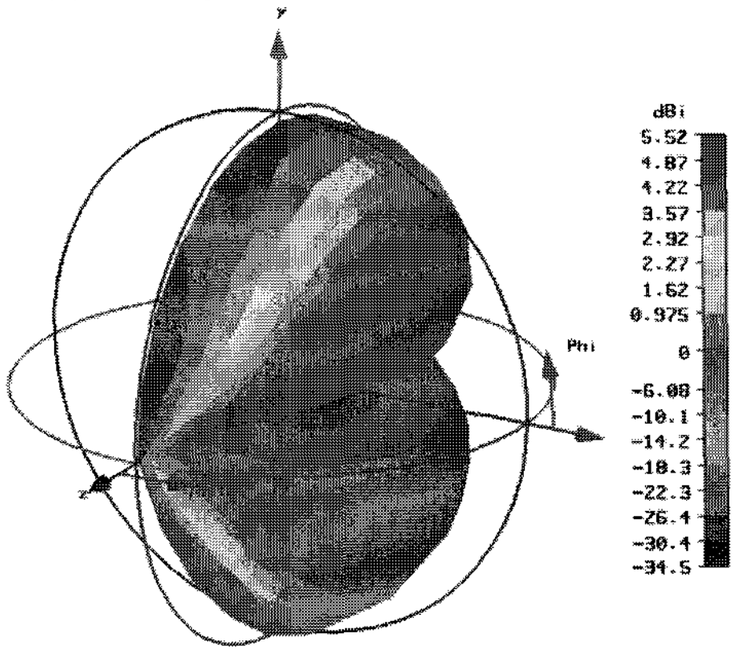

(b) Phi pattern of Far Field radiation

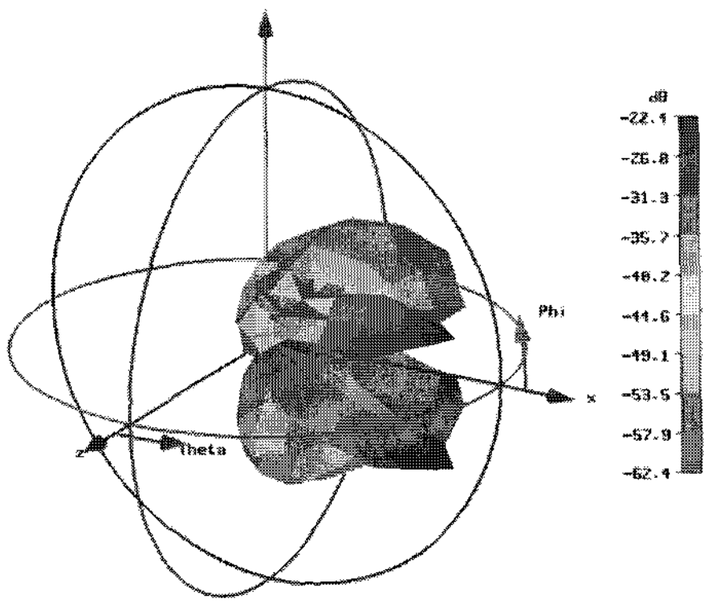

(c) Axial Ratio of far-field radiation pattern

Fig. 5. Far-field radiation pattern of UWB antenna sensor in CST MS studio version 5.0

The optimization parameters are Wn1, Wn2, Wf, and Ws with fixed feed line length Lf (see Fig. 1). The overall size of this structure is 40×30 mm2. The antenna has the following dimensions: Lg=8 mm, Ws=3mm, L1=23mm, Ln=13mm, Lf=14mm, Wn1=10mm, Wn2=22mm, and Wf = 1.7 mm.

To decide the resonant frequency band of the sensor the return loss parameter S11 is carried out by simulation. The final simulation result of return loss with the optimized parameters is indicated in Fig. 4.

The operating -10 dB bandwidth of the UWB sensor is from 460 MHz to 3.3GHz as presented in Fig. 4. It can also operate at -7dB of return loss at low frequency.

The radiation pattern is one of the most important characteristics of the antenna sensor. According to this radiation pattern, the location of sensors is decided as to which place can be dedicated from the diagnosis object to achieve the better sensitivity.

The radiation pattern of this UWB sensor is measured in the simulation and is shown in Fig. 5. This antenna sensor exhibits as a monopole directional antenna. Therefore it can easily point out the direction of the electromagnetic pulses coming from the PD source.

3. Experiment

3.1 Sensors Used in Experiment

In the experiment, the commercial high frequency current transformer sensor is used as a reference sensor to confirm partial discharge signal compared with our newly designed UWB sensor. HFCT, an inductive coupling device sensing the induced ground current caused by PD, can detect the frequency range of 2 to 40MHz.

The above simulated UWB sensor is fabricated by a photolithographic etching process, making the construction relatively easy and inexpensive to use with PCB FR4 dielectric material.

The 50Ω SMA connector is connected to the microstrip feed line in sensor fabrication and the fabricated sensor picture and HFCT picture used in the test are shown in Fig. 6 (a) and (b), respectively.

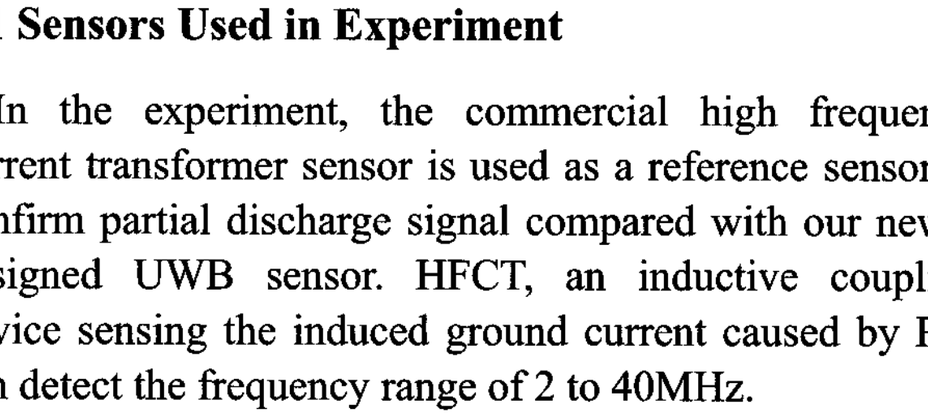

(a) (b)

Fig. 6. Picture of (a) HFCT sensor used in Test and (b) fabricated UWB sensor

3.2 Experiment Setup

We will investigate dismantled diagnosis on various kinds of discharge in stator winding insulation. In our laboratory testing, pre-made stator coils for corona discharge, surface discharge, and internal discharge, along with no defected stator winding, are injected by an external high voltage source. As shown in Fig. 7 (a) the internal discharge coil is specially made with some void defects inside the insulation and the surface discharge coil is made with a contaminated insulation surface. All stator coils except the corona discharge coil are injected by the external high voltage source without corona protection.

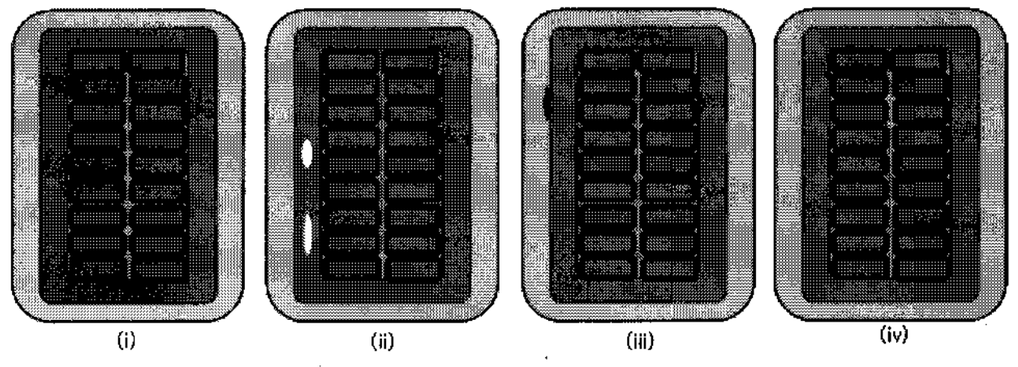

(a)

(b)

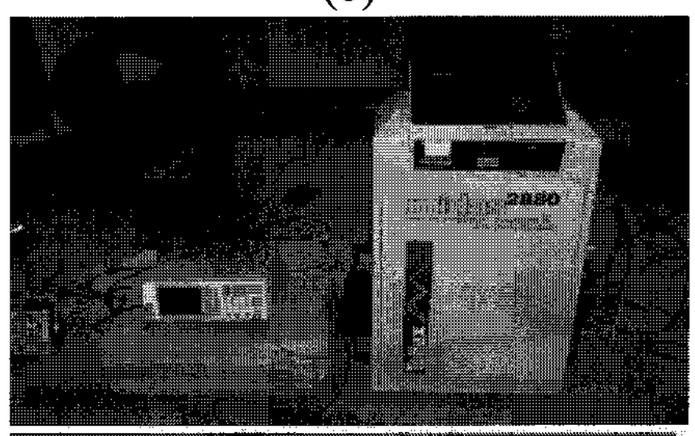

(c)

Fig. 7. (a) Pre-made discharge stator coil (i) normal discharge coil (ii) internal discharge (iii) surface discharge (iv) corona discharge (b) Picture of discharge coils and (c) Picture of Testing with High voltage source

These windings are dismantled from a 6.6kV rotating machine. A HFCT sensor is setup at the ground shield and its output and UWB sensor outputs are connected to a spectrum analyzer that gives the frequency domain results of the PD spectrum and connects to the digital oscilloscope to confirm PD signal in time domain and phase resolve partial discharge pattern (PRPD) in the high voltage cycle as shown in Fig. 8.

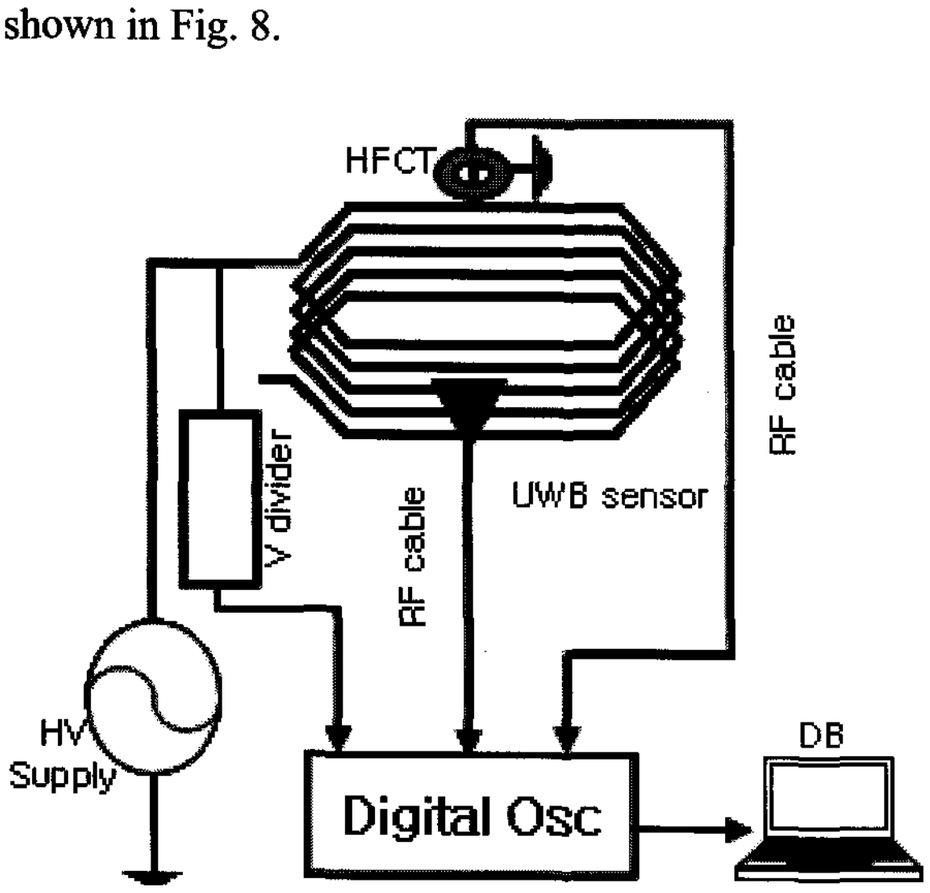

Fig. 8. Experimental setup in the laboratory

4. Test Results and Discussions

4.1 Time Domain Oscilloscope Results

In testing, the injection voltage is raised by the step of 0.5kV on each stator that is being made by particular discharge. The discharge signal can be occurred at 4.5kV on the corona discharge coil and surface discharge coil. The internal discharge coil starts discharge at 5.5kV. Therefore, all coils are injected at 4.5kV except the internal discharge coil which is discharged when 5.5 kV is injected in our experiment.

The experiment test results, measured with an oscilloscope, are displayed in Fig. 8. The detection of discharge activities are 2mV by HFCT and 3mV by UWB, 14 mV by HFCE and 10 mV by UWB sensor in the corona discharge coil, 5 mV by HFCT and 4 mV by UWB sensor in the surface discharge coil and 8 mV by HFCT and 5 mV by UWB sensor. All coils are injected at 4.5kV except the internal discharge coil which is injected at 5.5 kV.

4.2 Frequency Domain Spectrum

The output of the UWB sensor is measured by spectrum analyzer to check the frequency spectrum of the detected signal. 6.6kV is applied to each stator winding and the output partial discharge signal is measured with the spectrum analyzer. The signal spectrum of frequency range of 10MHz to 500MHz range is shown in Fig. 9.

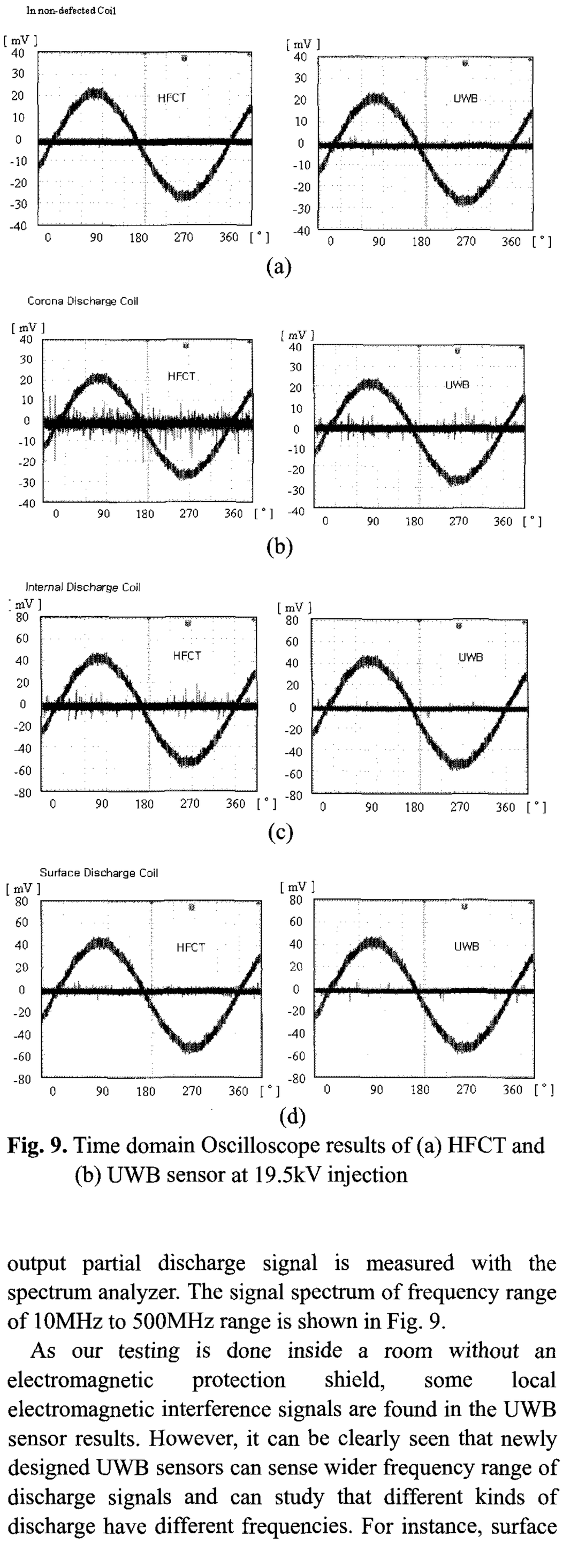

Fig. 9. Time domain Oscilloscope results of (a) HFCT and (b) UWB sensor at 19.5kV injection

As our testing is done inside a room without an electromagnetic protection shield, some local electromagnetic interference signals are found in the UWB sensor results. However, it can be clearly seen that newly designed UWB sensors can sense wider frequency range of discharge signals and can study that different kinds of discharge have different frequencies. For instance, surface

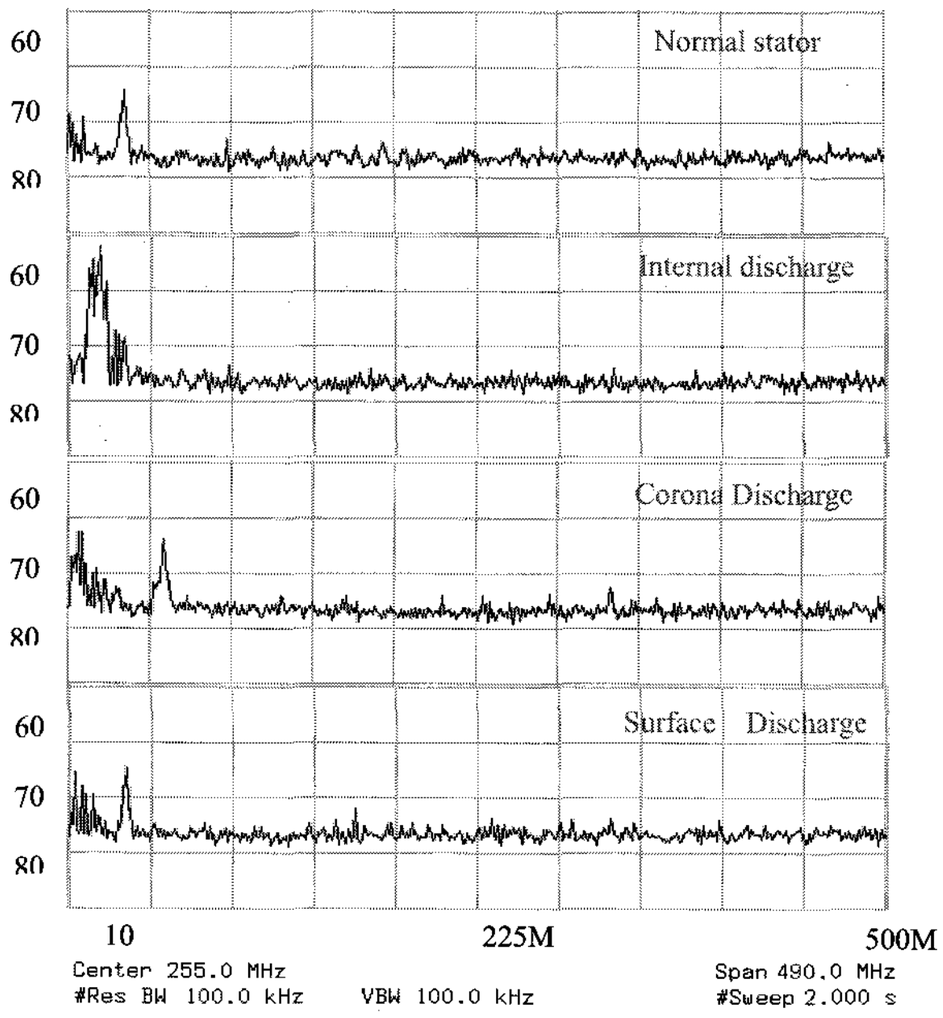

(a)

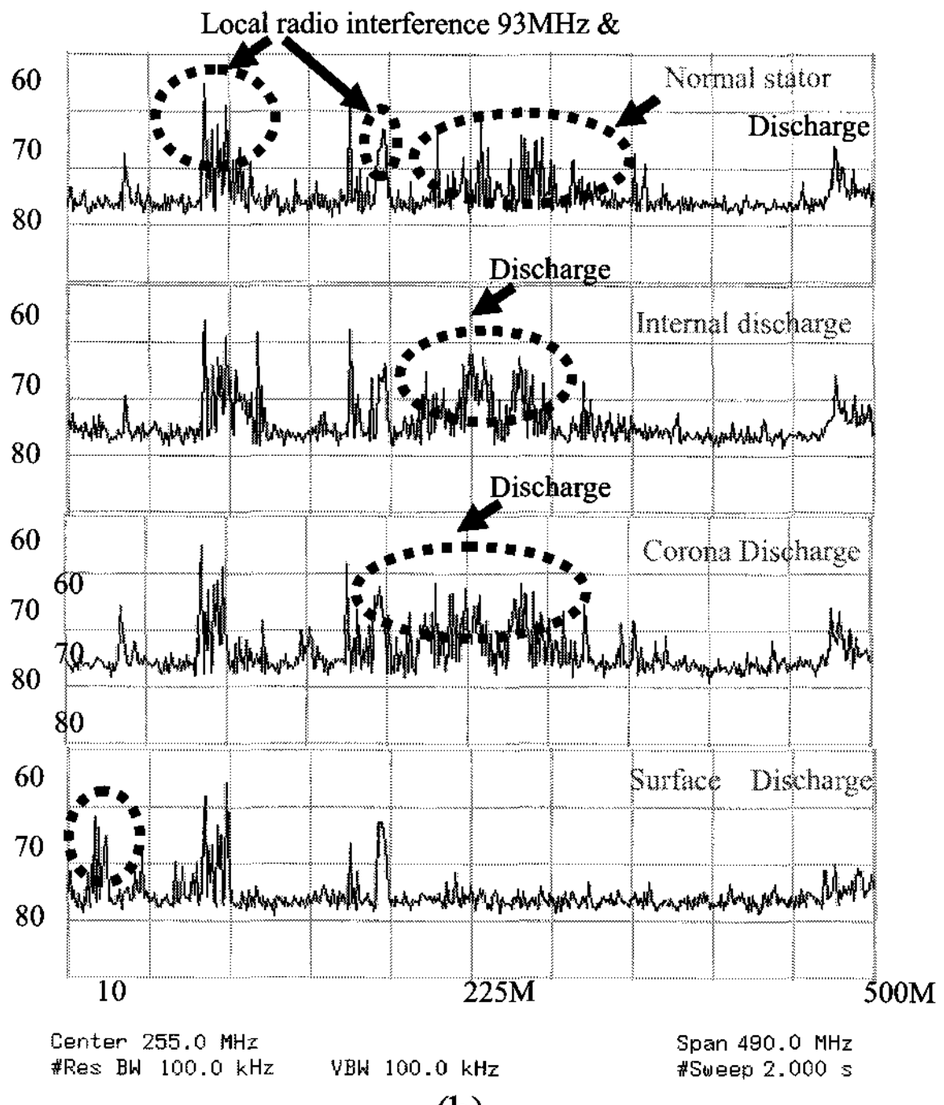

(b)

Fig. 10. Discharge signal spectrum detected by (a) UWB sensor (b) HFCT sensor

discharge, because of surface contamination, has very low frequency compared with other kinds of discharge.

The peak values of detected signals by HFCT and UWB sensors are compared as shown in Fig. 11. Although the sensitivity of the UWB sensor is lower than HFCT, the UWB sensor can detect both low frequency signal and high frequency region.

Therefore, the ultra wideband detection method is necessary to obtain the exact discharge signal energy or discharge quantity of both low frequency and high frequency bands.

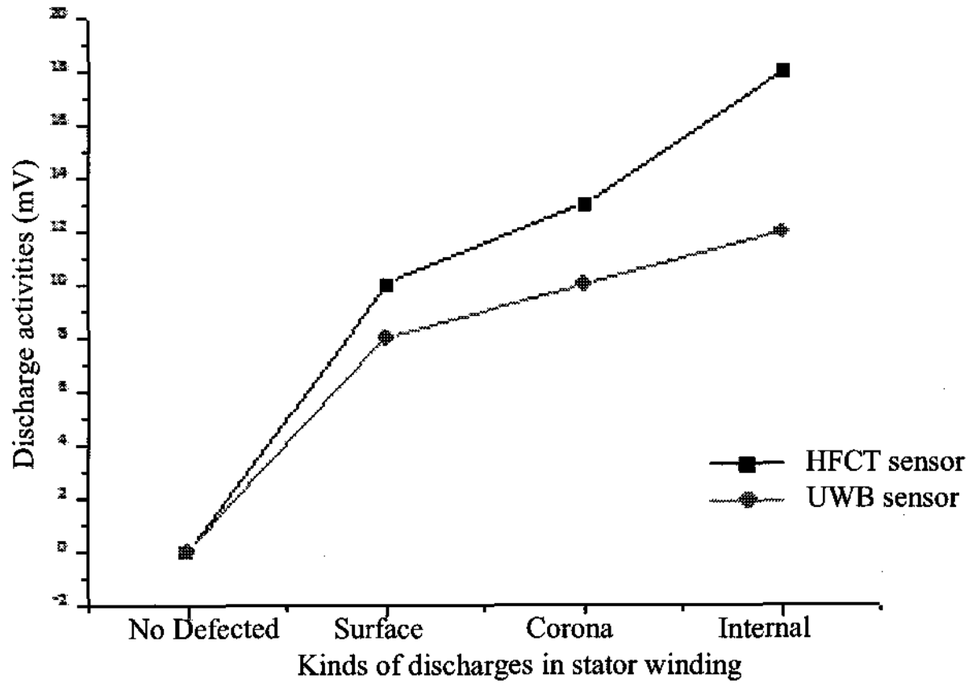

Fig. 11. Comparison of discharge activity of 4.5kV injection in oscilloscope detected by HFCT and UWB sensor for various kinds of discharge

5. Conclusion and Future Plan

As a conclusion, we verified that our new design of low frequency compact UWB sensor can also detect partial discharge signals compared with the commercial HFCT sensor. Furthermore, the newly designed UWB sensor can detect a very wide range of signal in both the low frequency and high frequency region. Furthermore, we studied discharge activities with different kinds of discharge in the stator winding insulation and found that the inception voltage of corona discharge and surface discharge are 4.5kV and inception voltage of internal discharge can be occurred at 5.5kV in a 6.6kV rated rotating machine.

Moreover, our new UWB sensor is small in size, light in weight and easy to integrate in the signal processing circuit and measuring system. Moreover it is easy to fabricate and cost effective. In the future, the study of frequency domain of the discharge signal will be made in detail and the study of ultra wideband PD signal will be carried out in total signal energy or discharge quantity by using the UWB sensor

Acknowledgment

This study has been sponsored by the Korea Electric Power Research Institute (R-2006-1-241-003) based on the support of the Electric Power Industry Technology Evaluation & Planning Dept.

Also, this work was financially supported by Brain Korea 21 program.

References

[1] *IEEE trial-use guide to the measurement of partial discharges in rotating machines*, IEEE-SA Standard Board, Apr. 2000.

[2] J. E. Timperly and E. K. Chambers, "Localization defects in large rotating machines and associated systems through EMI diagnosis," *CIGRE*, Paper 11-311, Sep. 1992.

[3] N. H. Ahmed and N. N. Srinivas, "Online partial discharge detection in cables," *IEEE trans. Diel. Elect. Insul.* vol. 5, no. 2, pp. 181-188, 1998.

[4] N. de Kock, B. Coric, and R. Pietsch, "UHF PD detection in GIS- suitability and sensitivity of the UHF method in comparison with the IEC 270 method," *IEEE Elect. Insul. Magazine*, vol. 12, no. 6, pp. 20-26, 1996.

[5] Masatake Kawada, "Ultra wideband UHF/VHF ratio interfereometer system for detecting partial discharge source," *IEEE Trans*, 2002.

[6] J. Jung, "A small wideband microstrip-fed monopole antenna," *Microwave Opt Technol Lett,* 15, 2005.

[7] S.-W. Su, K.-L. Wong, and C.-L. Tang, "Ultra wideband square planar monopole antenna for IEEE 802.16a operation in the 2-11GHz band," *Microwave Opt Technol Lett,* 42, 2004.

[8] J. Kim, "Design of an ultra wideband printed monopole antenna using FDTD and genetic algorithm," *IEEE microwave Wireless Compon Lett,* 12, 2002.

[9] R. Garg, P. Bhartia, I. Bahl, and A. Ittipiboon, *Microstrip antenna design handbook*, Artech House, 2000.

[10] Denissov, Ruben Grund, Thomas Klein, Wolfgang, Stefan Tenbohlen, "UHF partail discharge diagnosis of plug-in cable terminations," *Jicable*, 2007.

[11] D. M. Pozar and D. H. Schaubert, "Microstrip antenna: The analysis and design of microstrip antennas and arrays," *IEEE Express*, 1995.

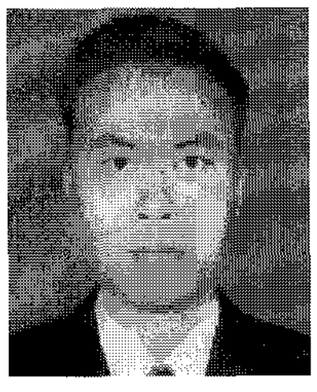

Kyaw Soe Lwin

He received the B.E degree in electronic engineering from Mandalay Technological University, Myanmar in 2001. And then he received M.E (electronic) degree in Yangon Technological University, Myanmar in 2005. Now he is studying Master Course at Department of Electrical, Elctronic & information Eng. in Wonkwang University, Korea. His interest includes EM sensing, diagnosis in high voltage insulation.

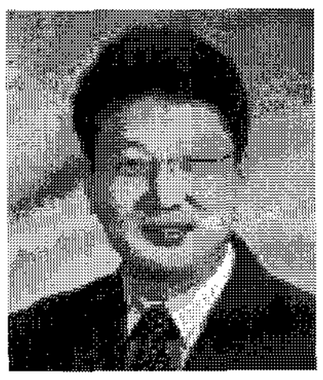

Noh-Joon Park

He received B.S., M.S. and Ph.D. degrees in Electronics Engineering from Wonkwang University in 1993, 1995 and 2004, respectively.

Since 2006, he has been a research professor with Center for Advanced Electric Applications at Wonkwang University working on design and analysis of EM sensors for partial discharge diagnosis in high voltage engineering, electronic circuit design with impedance matching technique for light sources.

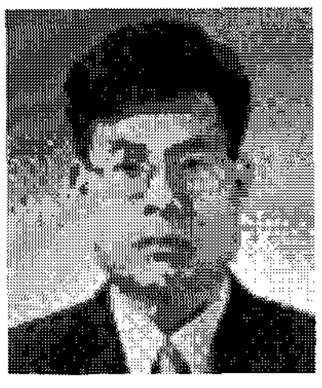

Hee-Dong Kim

He received the B.S, M.S and Ph.D. degrees in Electrical Engineering from Hongik University, Seoul, Korea, in 1985, 1987, and 1998, respectively. He is currently a principal researcher in the Power Generation Research Laboratory at Korea Electric Power Research Institute. He was a visiting researcher in the Department of Electrical Engineering, Kyushu Institute of Technology, Kitakyushu, Japan. His research interests are rotating machines, diagnostic tests, partial discharge, pulse propagation, electrical insulation, and continuous monitoring systems.

Young-Ho Ju

He received the B.S degree in Electrical Engineering from Inha University, Incheon, Korea, in 1981 and M.S degree in Electrical Engineering from Hanbat National University, Daejeon, Korea, in 2000. He is currently a chief researcher in the Power Generation Research Laboratory at Korea Electric Power Research Institute. His research interests are rotating machines, diagnostic tests, partial discharge, electrical insulation, and continuous monitoring systems.

Dae-Hee Park

He received B.S., M.S. degrees in Electrical Engineering from Hanyang University in 1979 and 1983, respectively and his Ph.D. degree from Osaka University in 1989. He worked at the LS Cable Research Institute as a Senior Researcher from 1979 to 1991. After that, he joined the School of Electrical, Electronics and Information Engineering at Wonkwang University where he is currently employed as a Professor. He was at MSU in the USA as a Visiting Professor from 1999 to 2000. His main research interests are in the areas of insulating and dielectric materials, LED lighting source and discharge.